

Pseudogap and antiferromagnetic correlations in the Hubbard model

Alexandru Macridin¹, M. Jarrell¹, Thomas Maier², P. R. C. Kent^{1,2} and Eduardo D'Azevedo²

¹ University of Cincinnati, Cincinnati, Ohio, 45221, USA

² Oak Ridge National Laboratory, Oak Ridge, Tennessee, 37831, USA

(Dated: August 21, 2018)

Using the dynamical cluster approximation and quantum monte carlo we calculate the single-particle spectra of the Hubbard model with next-nearest neighbor hopping t' . In the underdoped region, we find that the pseudogap along the zone diagonal in the electron doped systems is due to long range antiferromagnetic correlations. The physics in the proximity of $(0, \pi)$ is dramatically influenced by t' and determined by the short range correlations. The effect of t' on the low energy ARPES spectra is weak except close to the zone edge. The short range correlations are sufficient to yield a pseudogap signal in the magnetic susceptibility, produce a concomitant gap in the single-particle spectra near $(\pi, \pi/2)$ but not necessarily at a location in the proximity of Fermi surface.

Introduction – The normal state phase of high T_c superconductors at low doping, the pseudogap (PG) region, is characterized by strong antiferromagnetic (AF) correlations and a depletion of low energy states detected by both one and two-particle measurements[1]. Whereas the d-wave superconducting phase appears to be universal in the cuprates[2, 3], the PG region displays different properties in the electron and hole doped materials[4, 5]. In order to further develop a theory for high T_c superconductivity it is essential to have a better understanding of the asymmetry and similarities between the electron and the hole doped materials.

In the hole doped cuprates the antiferromagnetism is destroyed quickly upon doping (persisting to $\approx 2\%$ doping)[6] and the angle resolved photoemission spectra (ARPES) show well defined quasiparticles close to $(\pi/2, \pi/2)$ in the Brillouin zone (BZ) and gap states in the proximity of $(0, \pi)$ [4, 7, 8]. In the electron doped cuprates AF is more robust (persisting to $\approx 15\%$ doping)[9] and the ARPES at small doping ($\approx 5\%$) shows sharp quasiparticles at the zone edge and gap states elsewhere in the BZ[5, 8]. In the Hubbard model, or the closely related t-J model, the electron-hole asymmetry can be captured by including a finite next-nearest neighbor hopping t' [10, 11]. In this Letter we employ a reliable technique, the dynamical cluster approximation (DCA)[12, 13], on relatively large clusters, to investigate the PG and single-particle spectra at small doping, the asymmetry between electron and hole-doped systems, and the role of AF correlations on the PG physics.

We find that in the hole doped systems, the PG emerges in the proximity of $(0, \pi)$, requires only short range correlations, and its magnitude and symmetry is strongly influenced by t' . In the electron doped systems, the PG emerges along the diagonal direction, as a direct consequence of AF scattering, and requires long range AF correlations, but not necessarily long range order. The hopping t' enhances the AF correlations in the electron doped system and produces this AF gap. With reduced temperatures, the short range AF correlations suppress the low-energy spin excitations in both electron and hole

doped systems concomitant with the development of a single-particle gap in the proximity of $(\pi, \pi/2)$, but not necessarily with a PG close to the nodal or the antinodal points.

Formalism – The Hubbard Hamiltonian is

$$H = -t \sum_{\langle ij \rangle, \sigma} c_{i\sigma}^\dagger c_{j\sigma} - t' \sum_{\langle\langle il \rangle\rangle, \sigma} c_{i\sigma}^\dagger c_{l\sigma} + U \sum_i n_{i\uparrow} n_{i\downarrow}. \quad (1)$$

Here $c_{i\sigma}^{(\dagger)}$ destroys (creates) an electron with spin σ on site i and $n_{i\sigma}$ is the corresponding number operator. U is the on-site repulsion taken $U = W = 8t$ and t (t') is the (next) nearest-neighbors hopping. W is the electronic bandwidth. We keep the filling $n < 1$ and take $t' = -0.3t$ ($t' = 0.3t$)[14] to represent the hole (electron) doped cuprates. We present results for $n = 0.95$.

In the DCA[12] we map the original lattice model onto a periodic cluster of size $N_c = L_c \times L_c$ embedded in a self-consistent host. The correlations up to a range $\xi \lesssim L_c$ are treated accurately, while the physics on longer length-scales is described at the mean-field level. The reduction to an effective cluster model is achieved by coarse graining the BZ into N_c cells (see Fig.3 in Ref.[13]) and approximating the self-energy as a constant within each cell, $\Sigma(\mathbf{k}, \omega) \approx \Sigma(\mathbf{K}, \omega)$, where \mathbf{K} denotes the center of the cell which \mathbf{k} belongs to.

We solve the cluster problem using quantum Monte Carlo (QMC) [15]. We use two different 16 site cluster geometries[16, 17], 16A and 16B (see Fig.5 in Ref.[13]), which result in different coarse graining of the BZ. Calculations on larger clusters below the PG temperature and at large coupling ($U = W$) are not currently possible due to the QMC sign problem. The Maximum Entropy method[18] is employed to calculate the real frequency cluster Green's function from which the self-energy is extracted. The self-energy is interpolated using a smooth spline, and used to calculate the lattice spectrum $A(k, \omega)$. We find results identical to within error bars at all the common points of the coarse-grained BZ of the clusters. The result demonstrates that these 16 site clusters capture the momentum dependence of the self-energy rather

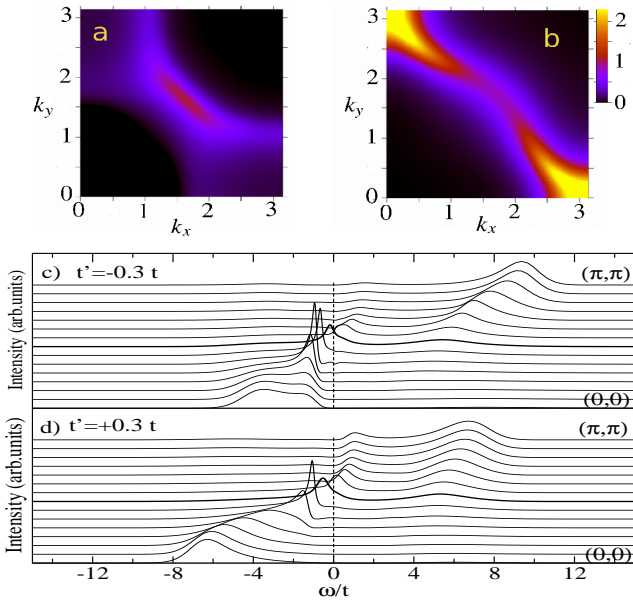


FIG. 1: (color) 5% doping, $T = 0.12t$. Zero energy surface $A(k, 0)$ for a) $t' = -0.3t$ and b) $t' = 0.3t$. $A(k, \omega)$ for k along the $(0, 0)$ - (π, π) direction in the BZ for c) $t' = -0.3t$ and d) $t' = 0.3t$.

well. We checked the robustness of our results at low temperature with calculations on smaller clusters where the sign problem is less significant.

Results – At a temperature $T_N = 0.19t$ ($0.24t$) for the hole (electron) doped system the AF correlation length reaches the cluster size yielding a divergent AF susceptibility (not shown). Below T_N one can proceed either by imposing the full symmetry on the effective medium, i.e. by reducing the problem to a cluster embedded in a paramagnetic (PM) host, or by allowing the host to develop long-range AF order. Both the PM and the AF solutions are complementary approximations to the exact solution: the first cuts off the AF correlations larger than the cluster size while the second introduces long range AF order via the mean-field character of the host.

Paramagnetic solution – In Fig. 1 -a and -b we show the spectral intensity at zero energy for the hole and electron doped systems, respectively. These plots are similar to the experimental ARPES data (see Fig.8 in Ref.[4] and Fig.3 in Ref.[5]). In both experiment and in our results, a region of large intensity can be observed close to $(\pi/2, \pi/2)$ and very low intensity is observed at the zone edge for hole doped systems. For the electron doped systems the intensity is maximum at $(0, \pi)$. However, the experimental data for the electron doped materials show gapped states along the diagonal direction [5]. In our calculations, Fig. 1 -b, the intensity at $(\pi/2, \pi/2)$ is similar to the one observed for the hole doped case and there is no PG along the zone diagonal. In fact $A(k, \omega)$ along the diagonal direction shows similar features for the hole and electron doped cases (Fig. 1-c and -d). Apart from the

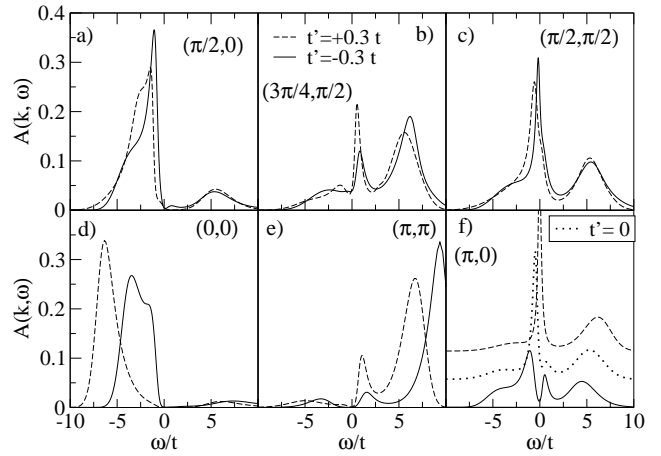


FIG. 2: $A(k, \omega)$ for different k points in the BZ for hole (full line) and electron (dashed line) doped cases, at 5% doping and $T = 0.12t$. In (f) the dotted line represents the spectrum for $t' = 0$.

differences at high energy close to the zone center and the zone corner which follow the non-interacting dispersion, the low-energy features along the zone diagonal are almost identical.

A comparison of the hole and electron spectra is presented in Fig. 2 and Fig. 3 -a, where $A(K, \omega)$ for K in the center of the cells which divide the BZ [26] are shown. In Figs. 2 -a, -b, -c and Fig. 3 -a, we find that the single particle spectra at low energy for the hole and the electron doped cases are surprisingly similar apart from the features close to $(0, \pi)$. In Fig. 2 -c we observe a sharp peak at $(\pi/2, \pi/2)$ in both the hole and electron doped spectra. Thus, there is no PG along the diagonal direction [27]. A particularly interesting feature, shown in Fig. 3 -a, is the depletion of the low energy states with lowering T in the proximity of $(\pi, \pi/2)$. Unlike the non-interacting case, where at $(\pi, \pi/2)$, there is only spectral weight for $\omega > 0$, there is now a broad feature with substantial weight at negative energies. This is due to AF scattering as can be deduced by comparing the main features with the $(\pi/2, 0)$ spectrum (Fig. 2 -a) found at the mirroring position with respect to AF zone boundary in the BZ. These shadow states develop a gap with decreasing temperature as shown in Fig. 3 -a where a large temperature spectrum ($T = 0.22t$, dotted line) and a low temperature one ($T = 0.12t$, dashed line) are plotted for the electron doped case. In literature the common description[19] of ARPES along the $(\pi, 0) - (\pi, \pi)$ cut is that the peak at $(\pi, 0)$ and $\omega < 0$ characterizing the PG evolves into a broad feature which loses intensity when approaching the zone corner. Our results indicate that the broad feature and gap at $(\pi, \pi/2)$ are not conditioned by the $(0, \pi)$ PG, being present in both electron and hole doped systems.

Differences between the hole and electron doped spectra are illustrated in Figs. 2 -d through -f. The high

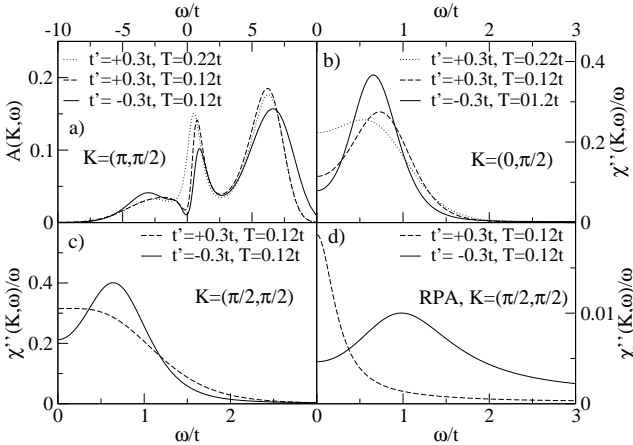


FIG. 3: 5% doping, hole doped (full line) and electron doped (dashed and dotted lines) cases. a) $A(k, \omega)$ at $k = (\pi, \pi/2)$. b) Low-energy dynamical spin susceptibility $\chi''(q, \omega)/\omega$ at $q = (0, \pi/2)$. The suppression of the spin excitations starts at the same temperature with the depletion of DOS at $(\pi, \pi/2)$, see dotted lines. c) $\chi''(q, \omega)/\omega$ at $q = (\pi/2, \pi/2)$. d) RPA results for $\chi''(q, \omega)/\omega$ at $q = (\pi/2, \pi/2)$.

energy features at zone center (Fig 2 -d) and zone corner (Fig 2 -e) are strongly influenced by t' . It is interesting that the position of these features seems to follow the non-interacting band structure, the energy difference between the non-interacting states at these points being about $8|t'|$. A fundamental difference between the electron and hole doped spectra at $(0, \pi)$ is shown in Fig. 2-f. The hole doped spectra exhibits a strong gap whereas the electron doped spectra has an intense peak. It is also worth looking at the $t' = 0$ case, shown in the figure with dotted line, where a PG is present but much less developed than the one for $t' = -0.3t$. Notice that even for the hole doped case (i.e. $t' < 0$) the magnitude of t' has a strong influence on symmetry with respect to zero energy of the density of states, which we believe to be important for interpreting tunneling experiments.

Aside from the depletion of DOS at the chemical potential, the PG is also associated with the suppression of the low-energy spin excitation[20]. For both electron and hole doped cases we find that the static spin susceptibility at $q = (0, 0)$ is strongly suppressed at temperatures below $T^* \approx 0.24t$, see Fig. 4-a. The momentum dependence of the dynamical spin susceptibility exhibits a dispersion similar to magnon one in the undoped anti-ferromagnets, with zero energy excitations at $q = (0, 0)$ and $q = (\pi, \pi)$, and gapped excitations at other q points in the BZ. For instance in Fig. 3 -b we show the imaginary part of the dynamical spin susceptibility, $\chi''(q, \omega)/\omega$ at $q = (0, \pi/2)$. In the electron doped case the position of the peak is found at larger energy which can be interpreted as a larger effective exchange interaction J and is consistent with stronger AF. What is interesting is that the suppression of the spin excitations and the

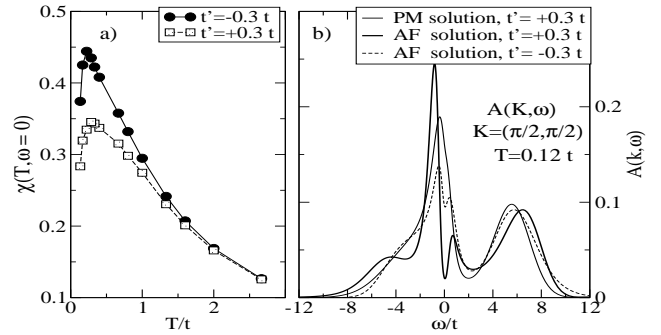


FIG. 4: a) Static spin susceptibility versus T . b) $A(k, \omega)$ averaged over the $(\pi/2, \pi/2)$ cell for the AF and the PM solutions.

formation of the remnant magnon peaks in $\chi''(q, \omega)/\omega$ is concomitant with the development of the gap in the single particle spectrum at $(\pi, \pi/2)$ (see Fig. 3 -a) and not necessarily imply a PG at $(0, \pi)$, observed only in the hole doped case, or elsewhere in the proximity of Fermi surface. However, the hole doped PG at $(0, \pi)$ is also coincident with the appearance of the remnant magnon peaks, indicating a short range AF correlations origin.

The spin excitation spectra are qualitatively similar for the electron and hole doped cases, but with a stronger suppression at low-energy in the hole doped case even though the AF is weaker. The largest difference can be observed at $q = (\pi/2, \pi/2)$ where at $T = 0.12t$ the hole doped spectra show a well developed gap whereas the electron doped one just starts to form (see Fig. 3 -d). This difference is a result of the corresponding differences in the ARPES, as can be concluded from Fig. 3 -d. Here the Random Phase Approximation (RPA) using the calculated $A(k, \omega)$ was employed for the calculation of the spin susceptibility. In this approximation the hole doped spin susceptibility at $(\pi/2, \pi/2)$ is gapped due to the gap at $(0, \pi)$ in the DOS which suppresses the excitations between the antinodal and the nodal points, unlike the electron doped susceptibility which is peaked at low-energy.

Antiferromagnetic solution – In Fig. 4 -b, we compare $A(k, \omega)$ for AF and PM cases. Here, a gap is obtained for the AF electron doped case close to $(\pi/2, \pi/2)$ in the BZ, in agreement with the experimental findings[5]. This gap is an AF gap and requires long range AF correlations. The short range AF correlations, of the order of a few lattice constants, are not sufficient to produce it. However, it is possible the PG to also appear in the PM state in large enough clusters that allow for long-range AF correlations. This conclusion is similar to the weak coupling PG mechanism predictions[21], even though in our case $U = W$. The hopping t' enhances the antiferromagnetism in the electron doped systems, producing the gap. Presumably any other parameters which favor the antiferromagnetism will have a similar effect. For ex-

ample, the AF solution for the hole doped case produces a gap at $(\pi/2, \pi/2)$ too, though a little smaller due to weaker antiferromagnetism. The spectral features away from $(\pi/2, \pi/2)$ within the AF solutions are not qualitatively different from the ones obtained with the PM solution (not shown). We note that the long range AF order does not yield a gap at $(0, \pi)$ for the electron doped case even though this point is on the AF zone boundary. The gap in DOS at $(\pi, \pi/2)$ developed in the PM solution is now enhanced by AF order, as well the intensity of the shadow states.

Our conclusions about the nature of the PG in the electron doped systems are different from those drawn from cluster perturbation theory (CPT)[21]. For $U \approx W$, CPT finds that, even when only short range AF correlations are considered, the states along the diagonal direction develop a gap, which persists even at large dopings $\approx 15\%$. Whereas in the experiment, at this doping value, the PG shows only at the intersection of the AF zone boundary with the non-interacting Fermi surfaces (hot spots)[22]. For agreement with experiment the authors of Ref.[21] proposed two different mechanisms for the PG in electron doped systems: a strong-coupling ($U \approx W$) PG at small doping produced by short range correlations and a weak-coupling ($U < W$) PG valid at intermediate doping which requires long range AF correlations. In contrast, we find no PG along the diagonal direction in the strong coupling regime unless long ranged AF correlations are considered, implying no need for two different PG mechanisms in the electron doped systems. A plausible reason for the discrepancy between the DCA and CPT results is the overestimation of AF correlations in the latter approach due to finite size effects[15] on small clusters[24] and lack of self-consistency[25].

We find that the inclusion in our calculation of a next-next-nearest-neighbor hopping $t'' \approx 0.2t$ [14] will not change the conclusions, this term having a rather small quantitative effect (though it may provide better agreement with experimental data). With *decreasing doping*, T^* increases but the number of available low-energy unoccupied states becomes smaller and therefore the PG features are more difficult to be resolved. With *increasing doping*, T^* decreases and the PG weakens, its features being hardly discernible above 15% doping. In the same time the $\omega < 0$ weight in the DOS at $(\pi, \pi/2)$ is reduced, indicating weaker AF scattering with increasing doping. In the AF solution the PG at larger doping will be located at the “hot spots”, even though the physics at those points requires fine k resolution and therefore is obtained from interpolation.

Conclusions – Using DCA we investigated the Hubbard model with next-nearest neighbor hopping t' . We find that: (1) The PG along the diagonal direction of the BZ in the electron doped systems is an AF gap which requires long range AF correlations. (2) The DOS in the proximity of $(0, \pi)$ is determined by the short range AF

correlations and it is strongly influenced by t' . For the hole (electron) doped systems t' yields a gap (an intense peak) at the zone edge. (3) Except in the proximity of $(0, \pi)$ the influence of t' on the low-energy ARPES is very weak. (4) t' has a strong influence on the high energy ARPES close to zone center and zone corner. (5) The magnitude of t' in the hole doped systems influences strongly the symmetry of the PG around the chemical potential. (6) The short range AF correlations suppress the low-energy spin susceptibility, produce remnant magnon peaks in the spin excitation spectra in both electron and hole doped systems and produce a gap in ARPES around $(\pi, \pi/2)$ but not necessarily in the proximity of the Fermi surface. When a $(0, \pi)$ PG is present in the ARPES, it emerges at the same temperature as the magnon peaks, suggesting a common origin of short ranged AF order. (7) Even though the antiferromagnetism is stronger in the electron doped case, the intense peak in DOS at $(0, \pi)$ hinders the suppression of low-energy spin excitations.

We thank George Sawatzky for useful discussions, and Kyle Shen and Donghui Lu for sharing their ARPES data. This research was supported by grants NSF DMR-0312680, NSF DMR-0113574, CMSN DOE DE-FG02-04ER46129 and NSF SCI-9619020 through resources provided by the San Diego Supercomputer Center. TM acknowledges support from the Center for Nanophase Materials Sciences, Oak Ridge National Laboratory, which is funded by the Division of Scientific User Facilities, U.S. Department of Energy.

- [1] T. Timusk and B. Statt, Rep. Prog. Phys. **62**, 61, (1999); M.R. Norman *et. al.*, Rep. Prog. Phys. **66**, 1547, (2003)
- [2] C. C. Tsuei *et. al.*, Phys. Rev. Lett. **73**, 593, (1994)
- [3] C. C. Tsuei *et. al.*, Phys. Rev. Lett. **85**, 182, (2000)
- [4] F. Ronning *et. al.*, Phys. Rev. B **67**, 165101, (2003)
- [5] N. P. Armitage *et. al.*, Phys. Rev. Lett. **88**, 257001, (2002).
- [6] Y. Kitaoka *et. al.*, J. Phys. Soc. Jpn. **56**, 3024 (1987).
- [7] B.O. Wells *et. al.*, Phys. Rev. Lett. **74**, 964 (1995)
- [8] A. Damascelli *et. al.*, Rev. Mod. Phys. **75**, 473 (2003).
- [9] G. M. Luke *et. al.*, Phys. Rev. B **42**, 7981 (1990).
- [10] T. Tohyama and S. Maekawa, Phys. Rev. B **49**, 3596 (1993), Supercond. Sci. Technol. **13**, R17, (2000); R. J. Gooding *et. al.* Phys. Rev. B **50**, 12866, (1994);
- [11] A. Macridin *et. al.* Phys. Rev. B **71**, 134527, (2005).
- [12] M. H. Hettler *et. al.* Phys. Rev. B **58**, R7475 (1998); M. H. Hettler *et. al.* Phys. Rev. B **61**, 12739 (2000);
- [13] Th. Maier *et. al.*, Rev. Mod. Phys. **77**, 1027 (2005).
- [14] O. Andersen *et. al.*, J. Phys. Chem. Solids **56**, 1573 (1995).
- [15] M. Jarrell *et. al.*, Phys. Rev. B **64**, 195130 (2001).
- [16] D. Betts *et. al.*, Can. J. Phys. **77**, 353 (1999).
- [17] P. R. C. Kent *et. al.*, Phys. Rev. B **72**, 060411 (2005).
- [18] M. Jarrell *et. al.*, Physics Reports **269** No.3, 133, (1996).
- [19] A. Ino *et. al.*, J. Phys. Soc. Jpn. **68**, 1496 (1999).
- [20] W. W. Warren *et. al.*, Phys. Rev. Lett. **62**, 1193 (1989); M. Takigawa *et. al.*, Phys. Rev. B **43**, 247 (1991); H.

Alloul *et al.*, Phys. Rev. Lett. **70**, 1171 (1993).

[21] D. Senechal *et al.*, Phys. Rev. Lett. **92**, 126401, (2004).

[22] N. P. Armitage *et. al*, Phys. Rev. Lett.**87**, 147003, (2001).

[23] B. Kyung *et al.*, Phys. Rev. Lett. **93**, 147004, (2004).

[24] T. Tohyama, Phys.Rev. **B** **70**, 174517 (2004).

[25] C. Gros and R. Valenti, Annalen der Phys. **3**, 469, (1994);
 D. Senechal *et al.*, Phys. Rev. Lett.**84**, 522,(2000)

[26] The self-energy in these K points results directly from DCA+MEM calculation. The self-energy in other K points is obtained by interpolation.

[27] We obtained the same conclusion from an 8 site cluster calculation where we could reach $T = 0.05t$ for $U = W$.